

# The Stress Detection and the Fatigue Lifetime of Stainless Steel AISI 316L during Three-Point Bending Cyclic Loading

M. Uhríčik<sup>1, a</sup>, M. Oravcová<sup>1</sup>, P. Palček<sup>1</sup>, M. Sapieta<sup>2</sup>, M. Chalupová<sup>1</sup>

<sup>1</sup> *University of Žilina, Faculty of Mechanical Engineering, Department of Materials Engineering, Slovakia*

<sup>1</sup> *University of Žilina, Faculty of Mechanical Engineering, Department of Applied Mechanics, Slovakia*

<sup>a</sup> *milan.uhricik@fstroj.uniza.sk*

**Abstract:** The article will describe investigation of the deformation of stainless steel during three-point bending cyclic loading with using thermovision. The analysis will prove different temperature response to external loading and dependence of elastic or plastic deformation development on material's state. The input data which are necessary for this analysis we will can get from temperature field of specimen surface. Process of elastic and plastic deformation is in dependence on radiation emitted by the object. For obtain thermal fields we will use thermal camera FLIR SC7000 with the highest sensitivity. The contribution also presents results of fatigue resistance of austenitic stainless steel AISI 316L, which is used as a biomaterial, obtained at low frequency cyclic loading in the high cycle fatigue region by three- point bending test. The fracture surface of the testing sample was examined using scanning electron microscopy (SEM).

**Keywords:** stainless steel; stress; three-point bending; fracture surface; thermal camera.

## 1 Introduction

Stainless steel is the name given to a family of corrosion and heat resistant steels containing a minimum of 10.5% chromium. Just as there is a range of structural and engineering carbon steels meeting different requirements of strength, weldability and toughness, so there is a wide range of stainless steels with progressively higher levels of corrosion resistance and strength. This variety of grades results from the controlled addition of alloying elements, each offering specific attributes in respect of strength and ability to resist different environments. To achieve the optimum economic benefit from using stainless steel, it is important to select a grade of steel which is adequate for the application without being unnecessarily highly alloyed and costly. Stainless steels can be classified into the five basic groups: austenitic stainless steels, duplex stainless steels, ferritic stainless steels, martensitic stainless steels and precipitation hardened steels [1-3].

Austenitic stainless steel AISI 316L has been used over decades as a metallic biomaterial as fracture repair devices and it has also a usage for making joint replacements. Their properties exceeds in good corrosion resistance, high biotolerance and suitable mechanical properties such as relatively high strength. Their corrosion resistance depends on Cr content and on the formation of a thin passive surface oxide layer. Austenitic stainless steel forms a single fcc austenite phase from its annealing temperature (~1050 °C) to room temperature and achieves its desirable strength and fatigue resistance through strain hardening and solid solution hardening mechanisms. These joint replacements are required to have a good combination of strength and ductility because they can undergo static or cyclic loading. Implant loading conditions are harsh because they occur in an aggressive body environment and that good corrosion-fatigue resistance is required too. Fracture can occur as a result of single overload or cyclic loading at stresses below the ultimate tensile strength and even below its yield strength. Fatigue failure is a process resulting first from change of mechanical properties, then fatigue crack initiation occurs and progressive growth of crack (propagation of fatigue crack) leading to final fracture. The failure can occur either in low number of cycles ( $\leq 10^4$  cycles; low cycle fatigue) or over millions of cycles (high cycle fatigue). The initiation of fatigue crack by cyclic loading is a result of dislocation interactions which lead to formation of micro voids and also dislocation run-

outs which create surface irregularities such as slip bands. These irregularities such as slip bands, inclusions, surface imperfections, grain boundaries and so on act as stress concentrators promoting local crack initiation [4-6].

Stress and fatigue testing are common test methods in mechanical engineering and materials science, but provide limited information on complex structures. Thermal stress mapping provides thousands of stress measurements simultaneously, even on geometrically complex components. The deformation of structural materials is followed by thermal effects. We recognize thermoelastic or thermoplastic stress analysis, depending on whether the load creates elastic or plastic strains. Thermoelastic stress analysis describes the relation between stress changes and temperature changes of a body in specimens [7]. Considering a three-point bend test, the stress is essentially zero at the neutral axis N-N. Stresses in the y axis in the positive direction represent tensile deformation, which increases, whereas stresses in the negative direction represent compressive deformation, it decreases. The thermoplastic effect quantifies the heat generated by plastic deformation. In the elastic part it is possible under adiabatic conditions to determine the value of the first stress invariant on the material surface by measuring changes of the surface temperature. The thermoelastic effect refers to the thermodynamic relationship between the change of stress in a component under elastic loading and the corresponding change of temperature. It is simply proportional to the change in the sum of the principal stresses, if adiabatic conditions prevail.

Thermoelastic and thermoplastic effect are summarized in a 3-dimensional heat equation together with the effect of heat conduction [7, 8]:

$$\rho C_\varepsilon \frac{\partial T}{\partial t} = k \left( \frac{\partial^2 T}{\partial x^2} + \frac{\partial^2 T}{\partial y^2} + \frac{\partial^2 T}{\partial z^2} \right) + T_0 \sum \frac{\partial \sigma_{ij}}{\partial T} \varepsilon_{ij}^e + \alpha_p \sigma_{ij} \varepsilon_{ij}^p \quad (1)$$

where

$\rho$	is the material density,
$C_\varepsilon$	is the specific heat capacity at constant deformation,
$T$	is the absolute temperature,
$t$	is the time,
$k$	is the thermal conductivity,
$x, y, z$	are spatial coordinates,
$T_0$	is the initial temperature,
$\sigma_{ij}$	is the stress tensor,
$\varepsilon_{ij}^e$	is the rate of change of elastic deformation,
$\alpha_p$	is the ratio of plastic deformation, which is converted to total heat of plastic deformation,
$\varepsilon_{ij}^p$	is the irreversible part of deformation tensor.

Thermoelastic effect is known as the conversion between mechanical forms of energy and heat. This transformation occurs when stress changes within a material element alter its volume. Density of energy generated in an object is transformed into local temperature changes. If specific heat of metal is high this phenomena is insignificant in terms of temperature change. Roughly 1 MPa change in stress state causes a temperature change of 1mK in steel [9, 10].

## 2 Experiment

For our analysis we used a commercially available type of austenitic stainless steel, especially AISI 316L. Its microstructure is shown in Figure 1 and its chemical composition is listed in the Tab. 1



Fig. 1: Microstructure of AISI 316L

Tab. 1: Chemical composition of AISI 316L.

Elements	C	Cr	Ni	Mo	Mn	Si	S	P
[%]	0.037	17.41	9.91	2.38	1.34	0.51	0.03	0.07

Stress and fatigue testing are common test methods in mechanical engineering and materials science, but provide limited information on complex structures. For three-point bending cyclic test, we used Vibrophores Amsler 150 HFP 5100 (Fig. 2a), which is using the resonance principle with constant or variable amplitude and mean load. The testing specimens were cut from rectangular bar to dimension of 10x10x55 mm and a V-notch was placed in the middle of the testing bars. First all the testing bars were preloaded with -6 kN and then cyclic loading was applied on the testing bars. After the test, the numbers of cycles were recorded as a dependence of frequency change from number of cycles for all the testing specimens.



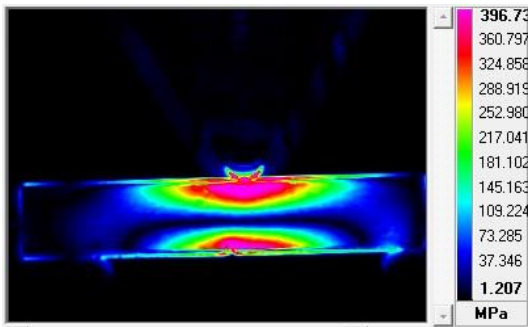
a) vibrophores Amsler 150 HFP 5100



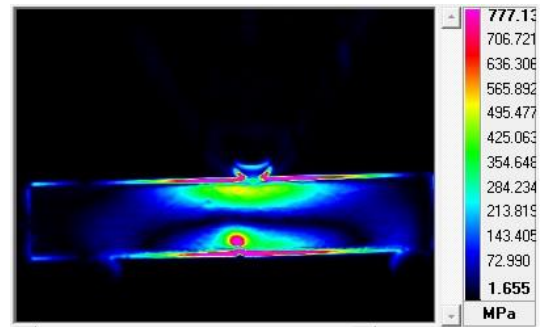
b) thermal camera FLIR SC7500

Fig. 2: Experimental equipment

Thermal stress mapping provides thousands of stress measurements simultaneously, even on geometrically complex components. The deformation of structural materials is followed by thermal effects. For obtain thermal fields we used thermal camera FLIR SC7500 (Fig. 2b). It is very flexible camera, with high sensitivity, accuracy, spatial resolution and speed. The results of monitoring fatigue test by thermal camera are shown in Figure 3a and Figure 3b.



a) at the beginning of the test



b) before the end of the test and after cracking

Fig. 3: Results from thermal camera for AISI 2136L during three-point bending test

### 3 Conclusion

The fracture's surface of the testing sample was observed by SEM. In Figure 4 is seen the macrophoto of the fracture area. After fatigue test, several initiation sites were observed under the notch, as shown in macroscopic view (Fig. 4). In Figure 5 is shown a detail of one initiation site. Also a line of cyclic deformation strengthening was observed on the fracture surface close to the final fracture. The fracture has mix fracture modes predominantly created by ductile separation with dimple morphology and also brittle intercrystalline facets, with the size of app.  $50 \times 90 \mu\text{m}$ , occur in the fracture and it can be seen in Figure 6 (with a detail of deformation strengthening line before final fracture in Figure 7). The intercrystalline facet was examined also on the opposite site of the sample's fracture as it can be seen in Figure 8 and Figure 9 where one site consists the salient and the opposite one consists the hollow.

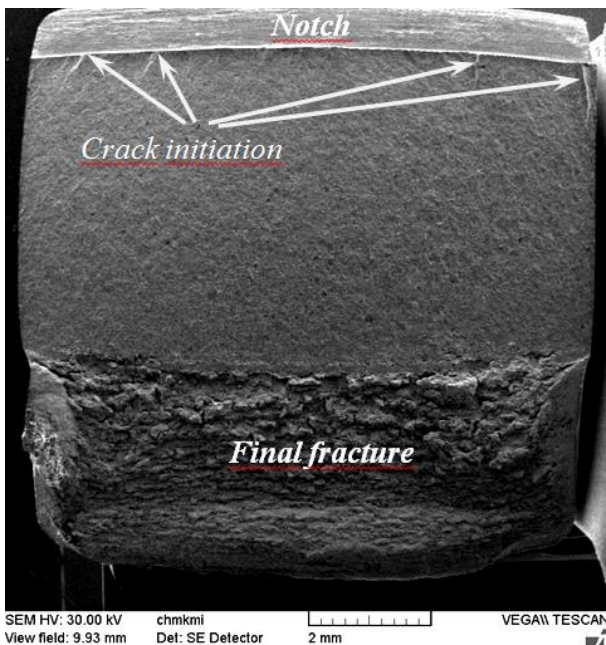


Fig. 4: Fracture surface of AISI 316L testing bar with several initiation sites, three-point bending fatigue

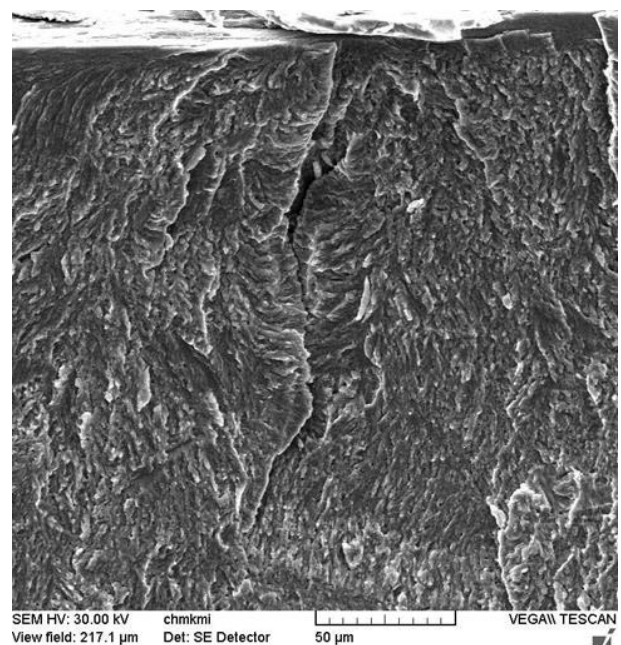


Fig. 5: Detail of one initiation site, AISI 316L, three-point bending fatigue

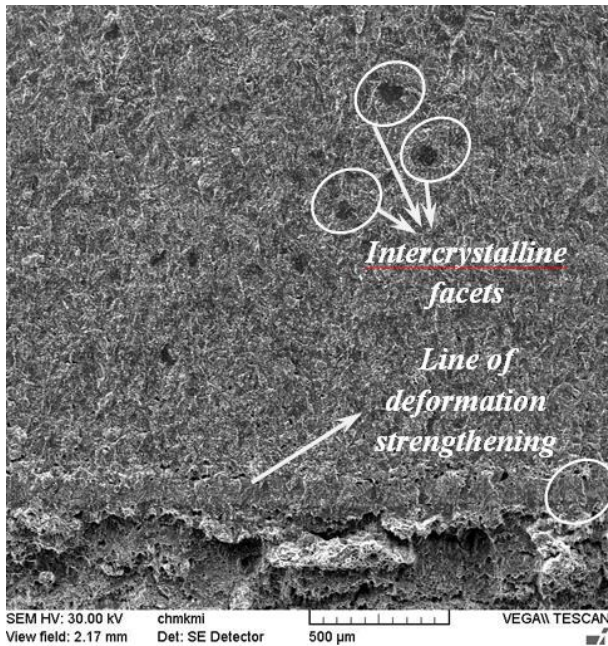


Fig. 6: Fracture surface of AISI 316L, intercrystalline fracture facets, deformation strengthening

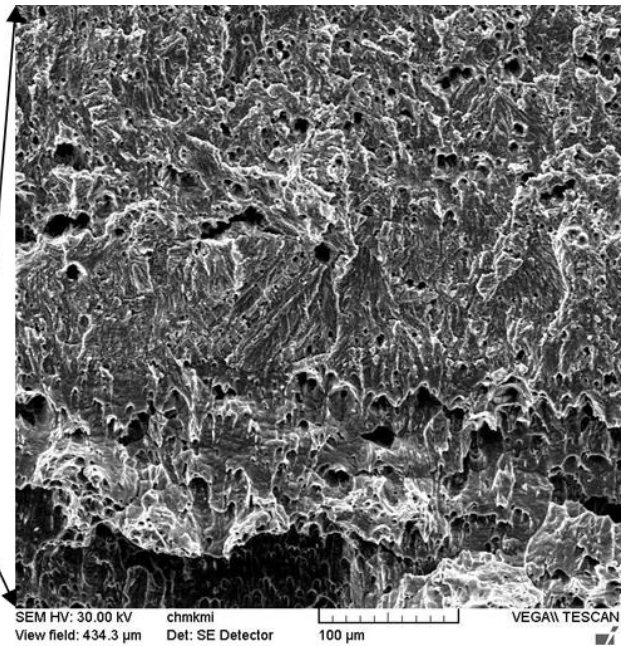


Fig. 7: Detail of deformation strengthening line before final fracture, AISI 316L

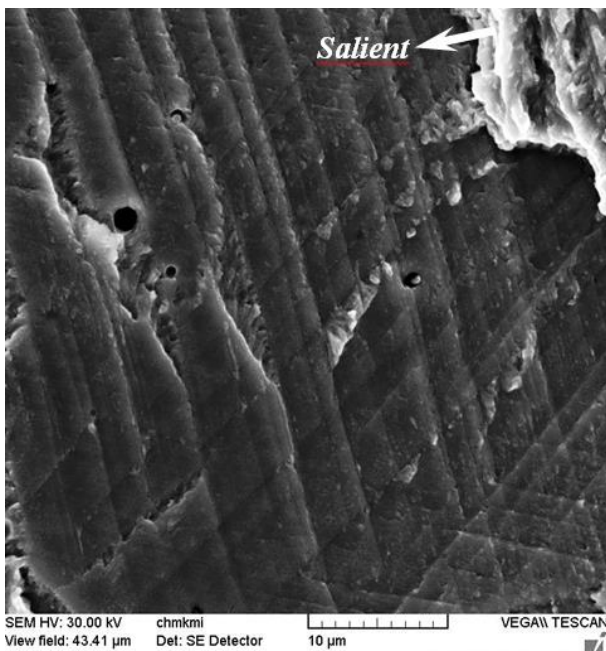


Fig. 8: Intercrystalline facet, right side of the sample

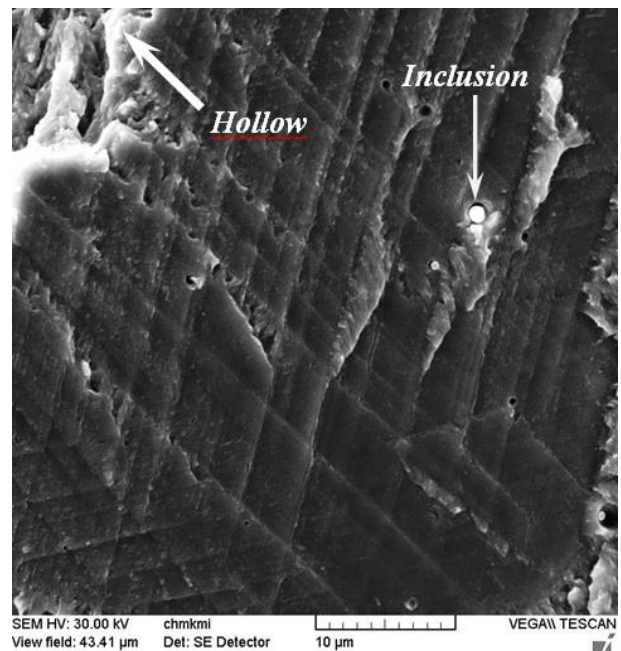


Fig. 9: Intercrystalline facet, left side of the sample

A crack was initiated on the testing bar by three-point fatigue bending test. The fracture has originated from several sites under the notch after  $412 \times 10^3$  cycles. The failure in the fracture surface was realized by ductile dimple fracture micromechanism. The dimple dimensions were in a range of 2 - 5 microns. In the fatigue area of the fracture surface the fracture was propagated by striation mechanism. Striation spacing in this area had grown in the range of 2 - 3 µm. The striations had soft corrugated surface. The numerous striations clearly state the fact that the testing sample has failed by fatigue. Inclusions of sulphate type were observed in the structure, mainly in the dimples. On the fracture's surface annealing twins were observed and also various intercrystalline facets with slip deformation.

By thermal camera, it can give good follow of fatigue crack initiation and its progress in the monitoring and evaluating of the fatigue lifetime of the material.

## Acknowledgement

This work has been supported by Scientific Grant Agency of Ministry of Education of Slovak Republic and Slovak Academy of Science, No.1/0683/15 and No.1/0533/15.

## References

- [1] K. V. Sudhakar, Metallurgical investigation of a failure in 316L stainless steel orthopaedic implant, Engineering Failure Analysis, Vol. 12, pp. 249-256, 2005.
- [2] M. E. Stevenson, M. E. Barkey, R. C. Bradt, Fatigue failures of austenitic stainless steel orthopedic fixation devices, ASM International, Vol. 2, No. 3, pp. 57-64, 2002.
- [3] F. Nový, V. Zatkalíková, O. Bokůvka, K. Miková, Gigacycle fatigue endurance of marine grade stainless steels with corrosion pits, Periodica Polytechnica: transportation engineering, Vol.41, No.2, pp.99-103, 2013.
- [4] V. Zatkalíková, L. Markovičová, J. Belan, T. Liptáková, Variability of local corrosion attack morphology of AISI 316Ti stainless steel in aggressive chloride environment, Manufacturing Technology, Vol.14, No.3, pp.493-497, 2014.
- [5] A. S. Lima, A. M. Nascimento, H. F. G. Abreu, P. Limaneto, Sensitization evaluation of the stainless steel AISI 304L, 316L, 321 and 347, Journal of Materials Science, volume 40, 2005.
- [6] L. Markovičová, L. Hurtalová, V. Zatkalíková, T. Garbacz, Evaluation of composite structures by light microscopy and image analysis, Manufacturing Technology, Vol.14, No.3, pp.351-355, 2014.
- [7] Z. Stankovičová, V. Dekýš, P. Novák, Z. Pelagić, Thermoelastic stress analysis – verification of experiment by using numerical simulation, Experimentální a výpočtové metody v inženýrství : II. Ročník conference pro mladé vědecké pracovníky, pp. 21, 2015
- [8] R. Plum, et al. Extended thermoelastic stress analysis applied to carbon steel and CFRP. [online]. 1999. Available online at: <<http://ebookbrowse.net/we5a3-pdf-d75918406>>.
- [9] P. Brémond. New developments in thermoelastic stress analysis by infrared thermography. [online]. 2007. Available online at: <<http://www.ndt.net/article/panndt2007/papers/138.pdf>>.
- [10] Z. Stankovičová, V. Dekýš, P. Novák, Thermal stress analysis of the specimen, Technológ, Vol. 7, No. 3, pp. 88-91, 2015.